JACS
JOURNAL OF THE AMERICAN CHEMICAL SOCIETY
pubs.acs.org/JACS
Article

Spin−Lattice Relaxation Decoherence Suppression in Vanishing Orbital Angular Momentum Qubits

Christian D. Buch, Krishnendu Kundu, Jonathan J. Marbey, Johan van Tol, Høgni Weihe, Stephen Hill, and Stergios Piligkos*

Cite This: J. Am. Chem. Soc. 2022, 144, 17597−17603
Read Online
ACCESS | Metrics & More | Article Recommendations | Supporting Information

ABSTRACT: Multifrequency electron paramagnetic resonance spectroscopy on oriented single crystals of magnetically dilute Gd(III) ions in $Gd_{0.004}Y_{0.996}$(trensal) is used to determine the Hamiltonian parameters of the ground $^8S_{7/2}$ term and its phase memory time, T_m, characterizing its coherent spin dynamics. The vanishing orbital angular momentum of the $^8S_{7/2}$ term makes it relatively insensitive to spin−lattice relaxation mediated by magnetoelastic coupling and leads to a T_m of 12 μs at 3 K, which is not limited by spin−lattice relaxation.

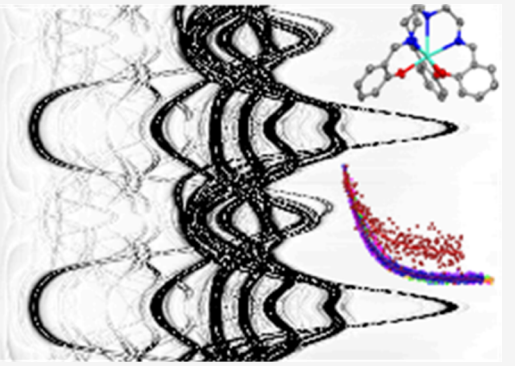

INTRODUCTION

We are currently experiencing the advent of quantum technologies, as defined within the context of the "second quantum revolution".[1−3] These emerging technologies, among which are quantum computing, simulators, communications, sensing, metrology, cryptography, and imaging, are based on the exploitation of genuine quantum properties of matter, such as superposition and entanglement. In particular, the realization of a general purpose quantum computer[4−8] (QC) is currently one of the most ambitious technological goals[9,10] since QCs will outperform classical computers (*Quantum Advantage*) for some specific types of computations, such as prime number factorization,[11] search of large databases,[12] and the accurate simulation of quantum many-body systems.[13] Attaining *Quantum Advantage* will change the way in which we process, search, and share information and will have a transformative impact on the development of novel materials and chemicals with applications in energy (magnets, batteries, superconductors), agriculture (efficient and sustainable fertilizers), and biomedicine and biotechnologies via the simulation of the conformational structures of proteins, leading to the discovery of new binding sites for custom-designed drugs or vaccines.

Very recently, superconducting and photonic quantum processing units (QPUs) were announced to have attained *Quantum Advantage*.[14−16] Although these are very impressive and encouraging achievements, the number of qubits included in these QPUs is still not sufficient to address practical problems, to which purpose the estimated number of incorporated qubits amounts to several thousands or even millions to be able to deal with quantum error correction.[17] Thus, the realization of future general purpose QCs will not be solely based on superconducting or photonic qubits but will require additional, or entirely different, components offering more efficient ways to fight against quantum error.

Molecular magnetic materials offer possibilities to circumvent some of these limitations and therefore constitute a very promising avenue for the next-generation *Quantum Information* technology devices.[18−23] Unlike many other candidates, molecular magnetic materials routinely display many low-energy states compatible with the encoding of qubits and even acting as integrated quantum processors, the additional levels providing the capability to expand the dimension of the computational space or to efficiently encode quantum error correction algorithms.[24−29] The critical parameter for the suitability of such materials to be used in *Quantum Information* devices is the phase memory time, T_m, reflecting the time for which the information encoding state retains its phase coherence.[30] Decoherence,[31] the interaction of the quantum system with its environment, results in loss of superposition and/or entanglement, collapsing the dynamic state of the system to its thermal equilibrium static eigenvectors. Strategies to reduce decoherence in molecular magnetic materials include

Received: July 6, 2022
Published: September 15, 2022

https://doi.org/10.1021/jacs.2c07057
J. Am. Chem. Soc. 2022, 144, 17597−17603

magnetic dilution to reduce magnetic dipolar interactions, isotopic enrichment to modify the nuclear spin composition of the environment, and chemically engineered systems displaying magnetic clock transitions (CTs). In the case of CTs, the vanishing magnetic field derivative of the energy of the information encoding states leads to insensitivity of the resonance frequency with respect to fluctuations of the local magnetic field and thus to an increased coherence of these states, reflected in their high T_m.[32,33] Furthermore, previous studies showed that the extent to which a quantum state is isotropic, or of S-character, is a factor affecting its T_m. In this context, divalent isotropic (or minimally anisotropic) d-shell ions were studied, targeting a ^2S ground term, resulting in T_ms of the order of microsecond.[34]

RESULTS AND DISCUSSION

Lanthanide (Ln) complexes are a rather unexplored but very interesting class of molecular spin qubits.[20,24,28,29,32,35,36] Some of us have recently demonstrated that the ground Kramers doublet of the $^2F_{7/2}$ ground term of the trigonally symmetric Yb(trensal)[37] is an excellent electronic qubit.[24] Yb(trensal) is also a prototypical coupled electronic qubit−nuclear qudit where efficient quantum error correction algorithms can intrinsically be implemented.[25] However, the orbital angular momentum ($L = 3$) of the $^2F_{7/2}$ term of Yb(III) limits its T_m via spin−lattice (SL) relaxation contributions to decoherence.[24,37] This prompted us to study Gd(trensal) since the ground $^8S_{7/2}$ term of Gd(III) is devoid of first-order orbital angular momentum with small high-order contributions from excited states possessing orbital angular momentum.[38] The ground $^8S_{7/2}$ term of Gd(III) mixes via spin−orbit coupling to primarily the $^6P_{7/2}$ and $^6D_{7/2}$ excited states, introducing at high order an orbital component to the ground $^8S_{7/2}$ term, reflected mainly in the splittings, and also g-factor, of c.w.-EPR spectra of Gd(III) ions.[38] However, as these excited states lie 33 000 and 40 000 cm^{-1} above the ground state, respectively, the amount of orbital momentum transmitted to the ground state is minimal, even for a relatively large spin−orbit coupling matrix element as in Gd(III).[38]

The energy spectrum of the ground $^8S_{7/2}$ term of Gd(III) due to the electrostatic potential of the ligands (ligand field, LF) and the Zeeman (ZE) interaction with the external magnetic field, $\vec{B}$, can phenomenologically be parameterized via the effective Hamiltonian

$$\hat{H} = \hat{H}_{LF} + \hat{H}_{ZE} = \sum_{k,-k\le q\le k} B_q^k \hat{O}_q^k + \mu_B \vec{B}\tilde{g}\hat{S} \quad (1)$$

where B_q^k and $\hat{O}_q^k$ are the Stevens parameters and operators, respectively, μ_B is the electron Bohr magneton, $\tilde{g}$ is the g-tensor, and $\hat{S}$ the spin angular momentum operator of the ground term. The SL interaction is mediated by vibrations that modulate the LF via magnetoelastic coupling terms. These terms, when considering their effect on the electronic functions to first order in displacement, are of the form[39]

$$\hat{H}_{SL} \propto \sum_i \frac{\partial \hat{H}_{LF}}{\partial R_i} \quad (2)$$

with ∂R being the displacement of the ith neighboring atom participating in the relevant vibration. Since $\hat{H}_{LF}$ expresses the electrostatic potential created by the ligands at the metal, it acts only on the orbital component of the eigenfunctions of the metal since this component expresses the charge distribution of the metal electrons. Thus, a vanishing orbital angular momentum component for the Ln functions leads to an insensitivity of the Ln center to SL relaxation via eq 2. This effect can be viewed as equivalent to magnetic CTs[32] where the resonance frequency is insensitive to local fluctuations of the magnetic field. Here, the resonance frequency is insensitive to local fluctuations of the LF. To assess the effect of the above on the coherent spin dynamics of the eigenstates of the $^8S_{7/2}$ term of Gd(III) in Gd(trensal), we first accurately determine the parameters entering (1) by multifrequency c.w.-EPR spectroscopy on single crystals and then probe the coherent spin dynamics of the ground $^8S_{7/2}$ term by pulse EPR spectroscopy.

As previously reported,[40−42] Gd(trensal), as other members of the Ln(trensal) family,[37,40−47] crystallizes in the $P\bar{3}c1$ space group as large pencil-shaped crystals in which the Gd(III) ion and the apical tertiary amine nitrogen atom (Figure 1) define

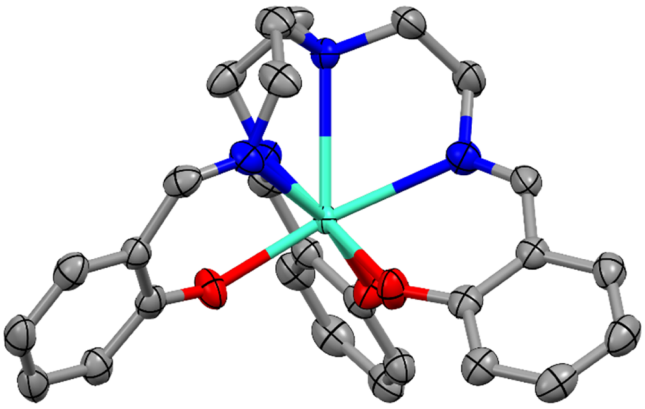

Figure 1. Molecular structure of Gd(trensal) determined by SCXRD. Hydrogens have been omitted for clarity. Color code: C, gray; N, blue; O, red; and Gd, cyan. Thermal ellipsoids are set to 90% probability.

the molecular C_3 axis and both lie on the crystallographic C_3 axis. Furthermore, two different molecular orientations are found along the trigonal crystallographic axis, corresponding to a relative rotation of two Gd(trensal) molecules by 48° around the C_3 axis (Figure S1). Gd(trensal) was magnetically diluted in its isostructural diamagnetic host, Y(trensal), at a 0.4% level [$Gd_{0.004}Y_{0.996}$(trensal), **1**], as determined by ICP-MS (Supporting Information (SI) section), to minimize dipolar interactions between paramagnetic Gd(III) centers. The c.w.-X-band EPR spectra of **1** at 15 K, with the magnetic field parallel or perpendicular to the C_3 axis, are shown in Figure 2a,b, respectively. A group of seven intense allowed lines centered around "$g = 2$" can be observed at both orientations. In addition, numerous lower-intensity forbidden lines, as well as "dimer" lines, originating from Gd(III) sites where the first neighbor is not a diamagnetic Y(III) center but rather a Gd(III), are observed. Similar "dimer" lines have been observed in both the c.w. and pulse EPR spectra of Yb(trensal).[24,37] Upon rotation of the crystal about an axis perpendicular to the C_3 axis, a splitting of each of the allowed lines is observed for all orientations where the magnetic field is not along the C_3 axis orientation or perpendicular to it. This is due to the two different molecular orientations in the crystal (Figure S1) being magnetically inequivalent at general orientations of the magnetic field. The angular dependence of the single-crystal X-band c.w.-EPR spectra of **1** in a plane

https://doi.org/10.1021/jacs.2c07057
J. Am. Chem. Soc. 2022, 144, 17597−17603

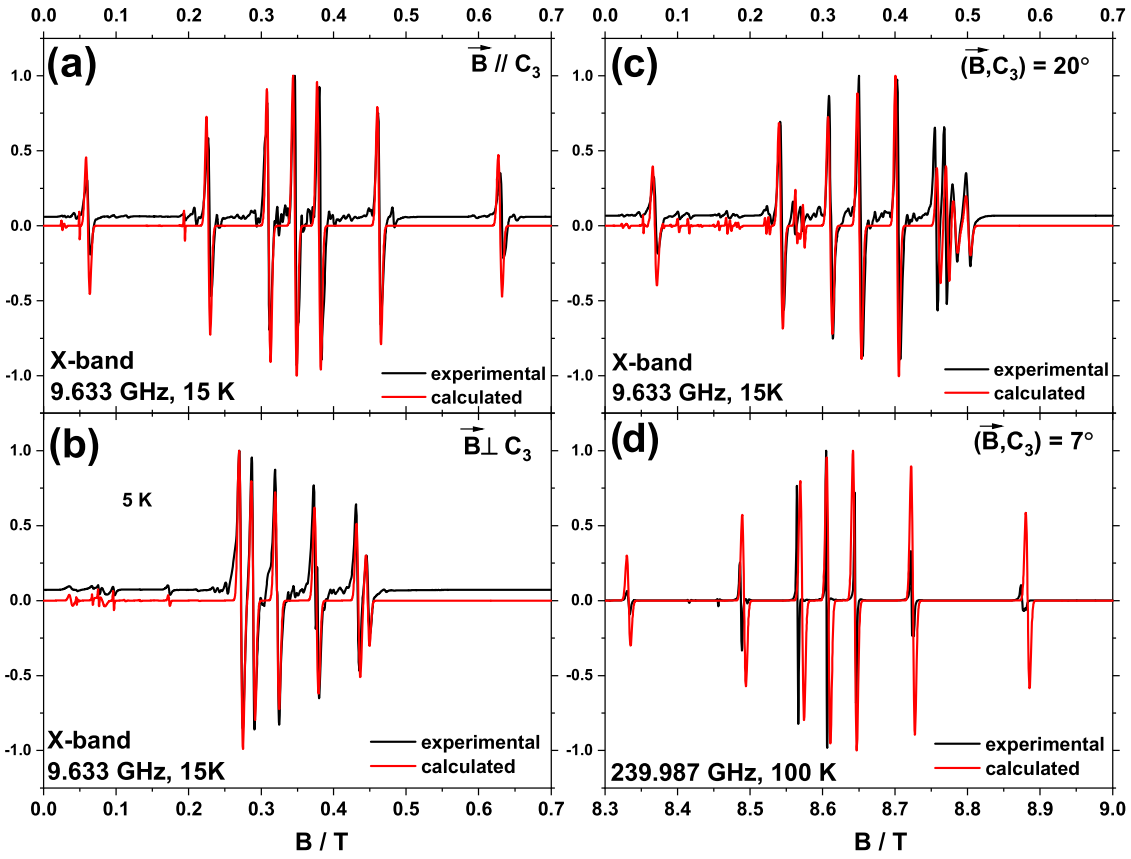

Figure 2. Multifrequency c.w.-EPR spectra on oriented single crystals of **1** at X-band and 240 GHz. Simulations were made as described in the text.

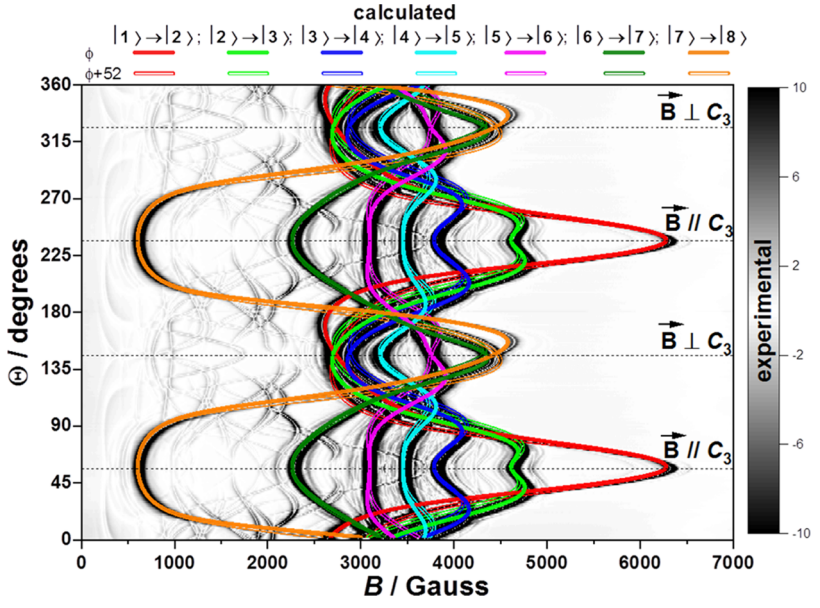

Figure 3. Angular variation of the X-band c.w.-EPR spectrum of **1** in a plane containing the C_3 axis and at 15 K. The |i⟩ labels refer to the eigenvectors given in Table S3. Simulations concern the allowed transitions.

containing the C_3 axis is shown in Figure 3. The determination of the parameters entering Hamiltonian (1) was performed by numerical fitting of the observed resonance fields by use of the Simplex algorithm.[48] Anticipating the discussion relevant to the determination of the relative splitting of the m_s sublevels of the $^8S_{7/2}$ term, we also recorded single-crystal c.w.-EPR spectra of **1** at higher frequency (240 GHz). When resonance fields of allowed transitions for an orientation of the magnetic field along C_3 (Figure 2a), close to it (Figure 2d), or perpendicular to C_3 (Figure 2b) are taken into account, only diagonal (k = 2,4,6; q = 0) Stevens parameters entering Hamiltonian (1), as well as the $g_{//}$ and $g_{\perp}$ factors, can be determined (Figure S2a,b,d). However, the use of only diagonal Stevens parameters fails to reproduce the spectra at intermediate

https://doi.org/10.1021/jacs.2c07057
J. Am. Chem. Soc. 2022, 144, 17597−17603

orientations (Figure S2c). Thus, to reproduce the observed resonance fields at general orientations of the magnetic field, the use of off-diagonal ($q \neq 0$) Stevens parameters is required. For this purpose, we also included in the fitting the observed X-band allowed transition resonance fields for an angle of the magnetic field of 20° with respect to the C_3 axis (Figure S3). This was done for one of the two magnetically inequivalent species (Figure S1). This resulted in the best-fit parameters: B_0^2 = +1.14 10^{-2} cm^{-1}, B_0^4 = + 4.84 10^{-5} cm^{-1}, B_0^6 = −6.07 10^{-9} cm^{-1}, B_3^4 = +5.79 10^{-4} cm^{-1}, B_{-3}^4 = −5.57 10^{-2} cm^{-1}, $g_{//}$ = 1.992, and $g_\perp$ = 1.985. The two off-diagonal parameters corresponding to real (q = 3) and imaginary (q = −3) matrix elements can be replaced by their vector sum in the complex plane. By imposing that this vector sum is a real number, one can reduce the number of parameters by one. Keeping the parameters entering (1) constant, a rotation of the laboratory coordinate frame by 52°, which is very close to 48°, which is the angle of the relative rotation of the two magnetically inequivalent species as defined by the C_3 axis and the phenolic oxygens (Figure S1), results in the reproduction of the resonant fields of the other magnetically inequivalent site (Figure 2c). Most importantly, the determined best-fit parameters excellently reproduce the full angular variation of the observed spectra at X-band for both allowed (Figure 3) and forbidden (Figure S4) transitions. The resulting energy level spectrum of the sublevels (Table S3) of the ground $^8S_{7/2}$ term with the obtained best-fit parameters (Figures S5 and S6) reveals that the smallest m_S projections are lowest in energy at zero magnetic field. To verify this result, we recorded the temperature dependence of the c.w.-EPR spectrum at 240 GHz (Figure S7) where significant depopulation effects can be observed, given the splitting of the $^8S_{7/2}$ term sublevels at zero magnetic field. The temperature dependence of the observed intensities (Figure S7) is in agreement with our assignment of the observed transitions.

The study and exploitation by magnetic resonance techniques of the spin dynamics of Ln coordination complexes, and more specifically of Gd-containing ones, are a vast research topic encompassing large research areas such as magnetic resonance imaging,[49] dynamic nuclear polarization,[50−54] and spin labeling for distance measurements,[54−58] an extensive review of which is outside the scope of this study. Thus, several previous investigations on frozen solutions or polycrystalline powders of Gd coordination complexes revealed that Gd(III) centers in such complexes display relatively long relaxation times and in some cases T_m's of the order of tens of microseconds. To probe the coherent spin dynamics of **1**, we measured pulse EPR spectra on single crystals of **1** at 240 GHz. The temperature dependence of the observed echo-detected field-swept (EDFS) spectra of **1** for an orientation of the applied magnetic field very close to the C_3 axis (Figure S8) reveals that EDFS spectra can be recorded for temperatures as high as 70 K. Hahn echo[59] and stimulated echo[60,61] sequences were used to determine the T_m and T_1 (Figures S9−S13), respectively, of the observed EDFS transitions. The determined parameters are given in Tables S4 and S5. At the lowest temperature (3 K), the T_m and T_1 of only the highest field transition can be determined because of the previously mentioned thermal depopulation effects at 240 GHz. At 3 K, we observe that the dynamic state described as a superposition of the two lowest sublevels (m_s = −5/2 and m_S = −7/2) of the $^8S_{7/2}$ term displays coherent spin dynamics characterized by a T_1 = 30 μs and by a phase memory time T_m = 12 μs (Table S4). The determined T_m is among the longest observed for purely f-electron molecular systems. By increasing the temperature (Figure 4), T_m decreases faster than T_1, indicating

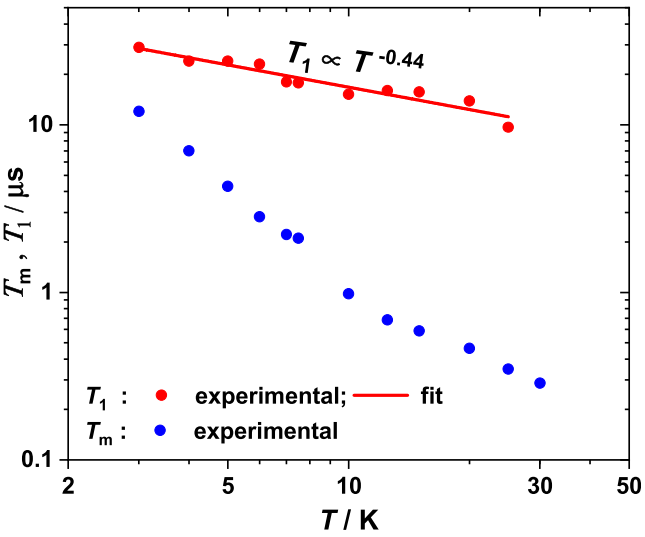

Figure 4. T_1 (red) and T_m (blue) at different temperatures. The measurements were performed at 240 GHz and 8.89 T for a single crystal of **1**, with the magnetic field oriented as described in the main text.

that coherent spin dynamics within the studied temperature and field range is not limited by spin−lattice-induced decoherence. The temperature dependence of T_1 is linear in a double log plot, indicating a power law $T_1 = DT^{-m}$, with m = 0.44 and D = 46.4 s $K^{-0.44}$, likely corresponding to a direct process that is promoted at high magnetic fields since for Kramers ions a direct process determined T_1 is inversely proportional to the fourth power of the external magnetic field, B.[39]

We have shown herein that long phase memory times can be achieved in purely f-electron systems essentially devoid of orbital angular momentum since local fluctuations of the LF cannot couple via magnetoelastic coupling terms to the wave functions of the electronic system. These results are in agreement with previous studies on d- or f-shell molecular systems where isotropic states, thus devoid of orbital angular momentum, have been probed.[20,34,62] Furthermore, they are also in agreement with recent experimental and theoretical studies[63] in which we demonstrated the importance of the magnetoelastic coupling and the role of the trigonal symmetry to the dynamic magnetic properties of the isostructural (displaying thus the same phonon spectrum) Yb(trensal) complex.[24] In addition, in previous coherent dynamics studies of Yb(trensal), we have shown that the ground term displays a phase memory time of a few hundred nanoseconds for $Yb_{0.07}Lu_{0.93}$(trensal) at X-band, which gets T_1 limited and of the order of 0.1 μs at around 20 K. Preliminary measurements on single crystals of $Yb_{0.01}Lu_{0.99}$(trensal) at 240 GHz (Figure S14) show similar T_m characteristics as those previously determined for Yb(III) at X-band.[24] In the case of Gd(trensal), the coherent spin dynamics is characterized by a T_m of 12 μs at 3 K and is still detectable at temperatures up to 70 K (Figure S8). Based on the results obtained herein and in previous studies,[20,34,62] a general strategy for the optimization of the coherence characteristics of molecular magnetic materials

https://doi.org/10.1021/jacs.2c07057
J. Am. Chem. Soc. 2022, 144, 17597−17603

should be based on the minimization of the partial derivatives of all parameters entering the time-dependent Hamiltonian of the systems.

■ ASSOCIATED CONTENT

Supporting Information

The Supporting Information is available free of charge at https://pubs.acs.org/doi/10.1021/jacs.2c07057.

> Crystallographic data (including structure factors) for Yb(trensal) have been deposited with the Cambridge Crystallographic Data Centre (CCDC 2183899). Copies of the data can be obtained, free of charge, on application to Cambridge Crystallographic Data Centre, 12 Union Road, Cambridge CB2 1EZ, UK (fax: +44-(0)1223-336033 or email: deposit@ccdc.cam.ac.uk) (PDF)

Accession Codes

CCDC 2183899 contains the supplementary crystallographic data for this paper. These data can be obtained free of charge via www.ccdc.cam.ac.uk/data_request/cif, or by emailing data_request@ccdc.cam.ac.uk, or by contacting The Cambridge Crystallographic Data Centre, 12 Union Road, Cambridge CB2 1EZ, UK; fax: +44 1223 336033.

■ AUTHOR INFORMATION

Corresponding Author

Stergios Piligkos − *Department of Chemistry, University of Copenhagen, DK-2100 Copenhagen, Denmark;* orcid.org/0000-0002-4011-6476; Email: piligkos@chem.ku.dk

Authors

Christian D. Buch − *Department of Chemistry, University of Copenhagen, DK-2100 Copenhagen, Denmark*

Krishnendu Kundu − *National High Magnetic Field Laboratory, Tallahassee, Florida 32310, United States*

Jonathan J. Marbey − *National High Magnetic Field Laboratory, Tallahassee, Florida 32310, United States*

Johan van Tol − *National High Magnetic Field Laboratory, Tallahassee, Florida 32310, United States*

Høgni Weihe − *Department of Chemistry, University of Copenhagen, DK-2100 Copenhagen, Denmark*

Stephen Hill − *National High Magnetic Field Laboratory, Tallahassee, Florida 32310, United States;* orcid.org/0000-0001-6742-3620

Complete contact information is available at: https://pubs.acs.org/10.1021/jacs.2c07057

Author Contributions

The manuscript was written through contributions of all authors. All authors have given approval to the final version of the manuscript.

Notes

The authors declare no competing financial interest.

■ ACKNOWLEDGMENTS

S.P. thanks the Novo Nordisk Foundation for research grant NNF20OC0065610. S.H. thanks the U.S. Department of Energy (under DE-SC0020260 to S.H.). Work performed at the NHMFL was supported by the U.S. National Science Foundation (DMR-1644779) and the State of Florida.

■ REFERENCES

(1) Riedel, M. F.; Bloch, I.; Debuisschert, T.; Wilhelm-Mauch, F.; Pruneri, V.; Vitanov, N. V.; Wehner, S.; Calarco, T. Europe's Quantum Flagship is taking off. *Europhys. News* **2018**, *49*, 30−34.

(2) Atzori, M.; Sessoli, R. The Second Quantum Revolution: Role and Challenges of Molecular Chemistry. *J. Am. Chem. Soc.* **2019**, *141*, 11339−11352.

(3) MacFarlane, A. G. J.; Dowling, J. P.; Milburn, G. J. Quantum technology: the second quantum revolution. *Philos. Trans. R. Soc., A* **2003**, *361*, 1655−1674.

(4) Feynman, R. P. Quantum-Mechanical Computers. *Found. Physiol.* **1986**, *16*, 507−531.

(5) Awschalom, D.; Samarth, N.; Loss, D. *Semiconductor Spintronics and Quantum Computation*; Springer: Berlin, 2002.

(6) Barnett, S. M. *Quantum information*; Oxford University Press: Oxford, 2009; Vol. *16*.

(7) Preskill, J. Quantum Computing in the NISQ era and beyond. *Quantum* **2018**, *2*, No. 79.

(8) Gibney, E. Physics: Quantum computer quest. *Nature* **2014**, *516*, 24−26.

(9) DiCarlo, L.; Reed, M. D.; Sun, L.; Johnson, B. R.; Chow, J. M.; Gambetta, J. M.; Frunzio, L.; Girvin, S. M.; Devoret, M. H.; Schoelkopf, R. J. Preparation and measurement of three-qubit entanglement in a superconducting circuit. *Nature* **2010**, *467*, 574−578.

(10) Thiele, S.; Balestro, F.; Ballou, R.; Klyatskaya, S.; Ruben, M.; Wernsdorfer, W. Electrically driven nuclear spin resonance in single-molecule magnets. *Science* **2014**, *344*, 1135−1138.

(11) Shor, P. W. Algorithms for quantum computation: discrete logarithms and factoring, 1994.

(12) Grover, L. K. Quantum Mechanics Helps in Searching for a Needle in a Haystack. *Phys. Rev. Lett.* **1997**, *79*, 325−328.

(13) Cirac, J. I.; Zoller, P. Goals and opportunities in quantum simulation. *Nat. Phys.* **2012**, *8*, 264−266.

(14) Arute, F.; Arya, K.; Babbush, R.; et al. Quantum supremacy using a programmable superconducting processor. *Nature* **2019**, *574*, 505−510.

(15) Wu, Y.; Bao, W. S.; Cao, S.; et al. Strong Quantum Computational Advantage Using a Superconducting Quantum Processor. *Phys. Rev. Lett.* **2021**, *127*, No. 180501.

(16) Zhong, H.-S.; Deng, Y. H.; Qin, J.; et al. Phase-Programmable Gaussian Boson Sampling Using Stimulated Squeezed Light. *Phys. Rev. Lett.* **2021**, *127*, No. 180502.

(17) Terhal, B. M. Quantum error correction for quantum memories. *Rev. Mod. Phys.* **2015**, *87*, 307−346.

(18) Rocha, A. R.; Garcia-Suarez, V. M.; Bailey, S. W.; Lambert, C. J.; Ferrer, J.; Sanvito, S. Towards molecular spintronics. *Nat. Mater.* **2005**, *4*, 335−339.

(19) Bogani, L.; Wernsdorfer, W. Molecular spintronics using single-molecule magnets. *Nat. Mater.* **2008**, *7*, 179−186.

(20) Gaita-Ariño, A.; Luis, F.; Hill, S.; Coronado, E. Molecular spins for quantum computation. *Nat. Chem.* **2019**, *11*, 301−309.

(21) Sessoli, R. All in one. *Nat. Phys.* **2021**, *17*, 1192−1193.

(22) Sessoli, R. Tackling the challenge of controlling the spin with electric field. *Natl. Sci. Rev.* **2021**, *8*, No. nwaa267.

(23) Bonizzoni, C.; Ghirri, A.; Santanni, F.; Atzori, M.; Sorace, L.; Sessoli, R.; Affronte, M. Storage and retrieval of microwave pulses with molecular spin ensembles. *npj Quantum Inf.* **2020**, *6*, 68.

(24) Pedersen, K. S.; Ariciu, A. M.; McAdams, S.; Weihe, H.; Bendix, J.; Tuna, F.; Piligkos, S. Toward Molecular 4f Single-Ion Magnet Qubits. *J. Am. Chem. Soc.* **2016**, *138*, 5801−5804.

(25) Hussain, R.; Allodi, G.; Chiesa, A.; Garlatti, E.; Mitcov, D.; Konstantatos, A.; Pedersen, K. S.; De Renzi, R.; Piligkos, S.; Carretta, S. Coherent Manipulation of a Molecular Ln-Based Nuclear Qudit Coupled to an Electron Qubit. *J. Am. Chem. Soc.* **2018**, *140*, 9814−9818.

(26) Gimeno, I.; Urtizberea, A.; Román-Roche, J.; Zueco, D.; Camón, A.; Alonso, P. J.; Roubeau, O.; Luis, F. Broad-band

spectroscopy of a vanadyl porphyrin: a model electronuclear spin qudit. *Chem. Sci.* **2021**, *12*, 5621−5630.
(27) Carretta, S.; Zueco, D.; Chiesa, A.; Gómez-León, Á.; Luis, F. A perspective on scaling up quantum computation with molecular spins. *Appl. Phys. Lett.* **2021**, *118*, No. 240501.
(28) Jenkins, M. D.; Duan, Y.; Diosdado, B.; García-Ripoll, J. J.; Gaita-Ariño, A.; Giménez-Saiz, C.; Alonso, P. J.; Coronado, E.; Luis, F. Coherent manipulation of three-qubit states in a molecular single-ion magnet. *Phys. Rev. B: Condens. Matter Mater. Phys.* **2017**, *95*, No. 064423.
(29) Martínez-Pérez, M. J.; Cardona-Serra, S.; Schlegel, C.; Moro, F.; Alonso, P. J.; Prima-García, H.; Clemente-Juan, J. M.; Evangelisti, M.; Gaita-Ariño, A.; Sesé, J.; van Slageren, J.; Coronado, E.; Luis, F. Gd-Based Single-Ion Magnets with Tunable Magnetic Anisotropy: Molecular Design of Spin Qubits. *Phys. Rev. Lett.* **2012**, *108*, No. 247213.
(30) Goldfarb, D.; Stoll, S. *EPR Spectroscopy: Fundamentals and Methods*; Wiley, 2018.
(31) Takahashi, S.; Tupitsyn, I. S.; van Tol, J.; Beedle, C. C.; Hendrickson, D. N.; Stamp, P. C. E. Decoherence in crystals of quantum molecular magnets. *Nature* **2011**, *476*, 76−79.
(32) Shiddiq, M.; Komijani, D.; Duan, Y.; Gaita-Ariño, A.; Coronado, E.; Hill, S. Enhancing coherence in molecular spin qubits via atomic clock transitions. *Nature* **2016**, *531*, 348−351.
(33) Kundu, K.; White, J. R. K.; Moehring, S. A.; Yu, J. M.; Ziller, J. W.; Furche, F.; Evans, W. J.; Hill, S. A 9.2-GHz clock transition in a Lu(II) molecular spin qubit arising from a 3,467-MHz hyperfine interaction. *Nat. Chem.* **2022**, *14*, 392−397.
(34) Ariciu, A.-M.; Woen, D. H.; Huh, D. N.; Nodaraki, L. E.; Kostopoulos, A. K.; Goodwin, C. A. P.; Chilton, N. F.; McInnes, E. J. L.; Winpenny, R. E. P.; Evans, W. J.; Tuna, F. Engineering electronic structure to prolong relaxation times in molecular qubits by minimising orbital angular momentum. *Nat. Commun.* **2019**, *10*, No. 3330.
(35) Aguilà, D.; Barrios, L. A.; Velasco, V.; Roubeau, O.; Repolles, A.; Alonso, P. J.; Sese, J.; Teat, S. J.; Luis, F.; Aromi, G. Heterodimetallic [LnLn'] Lanthanide Complexes: Toward a Chemical Design of Two-Qubit Molecular Spin Quantum Gates. *J. Am. Chem. Soc.* **2014**, *136*, 14215−14222.
(36) Luis, F.; Repolles, A.; Martinez-Perez, M. J.; Aguila, D.; Roubeau, O.; Zueco, D.; Alonso, P. J.; Evangelisti, M.; Camon, A.; Sese, J.; Barrios, L. A.; Aromi, G. Molecular Prototypes for Spin-Based CNOT and SWAP Quantum Gates. *Phys. Rev. Lett.* **2011**, *107*, No. 117203.
(37) Pedersen, K. S.; Dreiser, J.; Weihe, H.; Sibille, R.; Johannesen, H. V.; Sørensen, M. A.; Nielsen, B. E.; Sigrist, M.; Mutka, H.; Rols, S.; Bendix, J.; Piligkos, S. Design of Single-Molecule Magnets: Insufficiency of the Anisotropy Barrier as the Sole Criterion. *Inorg. Chem.* **2015**, *54*, 7600−7606.
(38) Wybourne, B. G. Energy Levels of Trivalent Gadolinium and Ionic Contributions to the Ground-State Splitting. *Phys. Rev.* **1966**, *148*, 317−327.
(39) Shrivastava, K. N. Theory of Spin−Lattice Relaxation. *Phys. Status Solidi B* **1983**, *117*, 437−458.
(40) Bernhardt, P. V.; Flanagan, B. M.; Riley, M. J. Completion of the Isomorphous Ln(trensal) Series. *Aust. J. Chem.* **2001**, *54*, 229−232.
(41) Habib, M.; Sain, S.; Das, B.; Chandra, S. K. Benign routes for the syntheses of polydentate Schiff base and their lanthanide complexes. *J. Indian Chem. Soc.* **2011**, *88*, 1501.
(42) Kanesato, M.; Yokoyama, T. Synthesis and Structural Characterization of Ln(III) Complexes (Ln = Eu, Gd, Tb, Er, Tm, Lu) of Tripodal Tris[2-(salicylideneamino)ethyl]amine. *Chem. Lett.* **1999**, *28*, 137−138.
(43) Kanesato, M.; Mizukami, S.; Houjou, H.; Tokuhisa, H.; Koyama, E.; Nagawa, Y. Comparison of the bond lengths for the lanthanide complexes of tripodal heptadentate ligands. *J. Alloys Compd.* **2004**, *374*, 307−310.
(44) Pedersen, K. S.; Ungur, L.; Sigrist, M.; Sundt, A.; Schau-Magnussen, M.; Vieru, V.; Mutka, H.; Rols, S.; Weihe, H.; Waldmann, O.; Chibotaru, L. F.; Bendix, J.; Dreiser, J. Modifying the properties of 4f single-ion magnets by peripheral ligand functionalisation. *Chem. Sci.* **2014**, *5*, 1650−1660.
(45) Kanesato, M.; Yokoyama, T.; Itabashi, O.; Suzuki, T. M.; Shiro, M. Synthesis and Structural Characterization of Praseodymium(III) and Neodymium(III) Complexes of Tripodal Tris[2-(salicylideneamino)ethyl]amine. *Bull. Chem. Soc. Jpn.* **1996**, *69*, 1297−1302.
(46) Kanesato, M.; Yokoyama, T. Crystal Structures of Dysprosium-(III) and Holmium(III) Complexes of Tripodal Tris[2-(salicylideneamino)ethyl]amine. *Anal. Sci.* **2000**, *16*, 335−336.
(47) Bernhardt, P. V.; Flanagan, B. M.; Riley, M. J. Isomorphous Lanthanide Complexes of a Tripodal N4O3 Ligand. *Aust. J. Chem.* **2000**, *53*, 229−231.
(48) Press, W. H.; Teukolsky, S. A.; Vetterling, W. T.; Flannery, B. P. *Numerical Recipes in C: The Art of Scientific Computing*, 2nd ed.; Cambridge University Press: Cambridge, 1992.
(49) Wahsner, J.; Gale, E. M.; Rodríguez-Rodríguez, A.; Caravan, P. Chemistry of MRI Contrast Agents: Current Challenges and New Frontiers. *Chem. Rev.* **2019**, *119*, 957−1057.
(50) Corzilius, B.; Smith, A. A.; Barnes, A. B.; Luchinat, C.; Bertini, I.; Griffin, R. G. High-Field Dynamic Nuclear Polarization with High-Spin Transition Metal Ions. *J. Am. Chem. Soc.* **2011**, *133*, 5648−5651.
(51) Stevanato, G.; Kubicki, D. J.; Menzildjian, G.; Chauvin, A.-S.; Keller, K.; Yulikov, M.; Jeschke, G.; Mazzanti, M.; Emsley, L. A Factor Two Improvement in High-Field Dynamic Nuclear Polarization from Gd(III) Complexes by Design. *J. Am. Chem. Soc.* **2019**, *141*, 8746−8751.
(52) Kaushik, M.; Qi, M.; Godt, A.; Corzilius, B. Bis-Gadolinium Complexes for Solid Effect and Cross Effect Dynamic Nuclear Polarization. *Angew. Chem., Int. Ed.* **2017**, *56*, 4295−4299.
(53) Capozzi, A.; Patel, S.; Wenckebach, W. T.; Karlsson, M.; Lerche, M. H.; Ardenkjær-Larsen, J. H. Gadolinium Effect at High-Magnetic-Field DNP: 70% 13C Polarization of [U-13C] Glucose Using Trityl. *J. Phys. Chem. Lett.* **2019**, *10*, 3420−3425.
(54) Nagarajan, V.; Hovav, Y.; Feintuch, A.; Vega, S.; Goldfarb, D. EPR detected polarization transfer between Gd3+ and protons at low temperature and 3.3 T: The first step of dynamic nuclear polarization. *J. Chem. Phys.* **2010**, *132*, No. 214504.
(55) Goldfarb, D. Gd3+ spin labeling for distance measurements by pulse EPR spectroscopy. *Phys. Chem. Chem. Phys.* **2014**, *16*, 9685−9699.
(56) Giannoulis, A.; Ben-Ishay, Y.; Goldfarb, D. *Methods Enzymol*, Cotruvo, J. A., Ed.; Academic Press, 2021; Vol. *651*, pp 235−290.
(57) Raitsimring, A. M.; Gunanathan, C.; Potapov, A.; Efremenko, I.; Martin, J. M. L.; Milstein, D.; Goldfarb, D. Gd3+ complexes as potential spin labels for high field pulsed EPR distance measurements. *J. Am. Chem. Soc.* **2007**, *129*, 14138−14139.
(58) Yagi, H.; Banerjee, D.; Graham, B.; Huber, T.; Goldfarb, D.; Otting, G. Gadolinium Tagging for High-Precision Measurements of 6 nm Distances in Protein Assemblies by EPR. *J. Am. Chem. Soc.* **2011**, *133*, 10418−10421.
(59) Hahn, E. L. Spin Echoes. *Phys. Rev.* **1950**, *80*, 580−594.
(60) Takahashi, S.; van Tol, J.; Beedle, C. C.; Hendrickson, D. N.; Brunel, L.-C.; Sherwin, M. S. Coherent Manipulation and Decoherence of $S=10$ Single-Molecule Magnets. *Phys. Rev. Lett.* **2009**, *102*, No. 087603.
(61) Schweiger, A.; Jeschke, G. *Principles of Pulse Electron Paramagnetic Resonance*; Oxford Univeristy Press: New York, 2001.
(62) Handzlik, G.; Magott, M.; Arczyński, M.; Sheveleva, A. M.; Tuna, F.; Sarewicz, M.; Osyczka, A.; Rams, M.; Vieru, V.; Chibotaru, L. F.; Pinkowicz, D. Magnetization Dynamics and Coherent Spin Manipulation of a Propeller Gd(III) Complex with the Smallest Helicene Ligand. *J. Phys. Chem. Lett.* **2020**, *11*, 1508−1515.
(63) Kragskow, J. G. C.; Marbey, J.; Buch, C. D.; Nehrkorn, J.; Ozerov, M.; Piligkos, S.; Hill, S.; Chilton, N. F. Analysis of vibronic

coupling in a 4f molecular magnet with FIRMS. *Nat. Commun.* **2022**, *13*, No. 825.

https://doi.org/10.1021/jacs.2c07057
J. Am. Chem. Soc. 2022, 144, 17597−17603